Oscillations induced by different timescales in signal transduction modules regulated by slowly evolving protein-protein interactions

I. Ndiaye, M. Chaves* and J.-L. Gouzé

Abstract

The dynamics induced by the existence of different timescales in a system is explored, in the context of a model composed of activation and signalling modules regulated by a slowly evolving process, such as some particular protein-protein interactions or genetic-like dynamics. It is shown that slowly varying regulation patterns can induce rapid changes in the steady states of the (fast varying) signal transduction pathway, and lead to sustained oscillations. These results are illustrated by a reduced model of the cdc2-cyclin B cell cycle oscillator. Using available experimental data, parameters of the model are estimated and found to agree with the requirements for a mechanism for oscillatory behaviour arising from coupling fast and slow processes.

1 Introduction

Signalling pathways are fundamental modules of intercellular organization and regulation. They are responsible for transmitting information from the exterior to the interior of the cell (or between two intercellular regions), along signal transduction cascades. Signalling pathways frequently interact among each other or with gene expression, to regulate cellular functions, in response to external stimuli. For instance, gene transcription is often the ultimate result of signalling events but, conversely, changes in gene expression patterns can also activate a signal transduction cascade. In general, signal transduction pathways and gene networks operate at different timescales. Typical signalling times are on the order of seconds, a fast process when compared to gene expression patterning, which may range from minutes to hours (see, for instance, Table 2.1 in [1]).

In this paper, we study a general system with three components: an activation module, a signalling module and a slowly evolving regulatory module. The activation and signalling components are considered fast relative to the regulatory component. In this system, the signalling module has two stable modes of operation (which correspond to two steady states for a fixed concentration of the regulatory component). We show how the signalling module can be regulated between its two stable modes of operation by a slowly varying (*e.g.*, genetic) pattern. In particular, we study the interaction between components with different timescales – slow (genetic-like) component and fast signalling component – which may induce oscillations in the concentrations of the system's mRNAs and proteins.

Examples of biological systems where an interaction between genetic and signalling (or two signalling) modules leads to oscillatory behaviour include the p53-mdm2 [2] or the IκB-NFκB networks [3]. We will consider 3- and 2-dimensional models as represented schematically in Fig. 1.   Our models were inspired by signal transduction cascades (such as MAPK cascades [4, 5]), and, more particularly, by a model of the cdc2-cyclin B cell cycle oscillator proposed in [6, 7]. This system plays an important role in the progression from G2 to M phases in the early embryonic cell cycle in *Xenopus laevis* oocytes. Cdc2 (a cell division cycle protein; represented by x_0 in Fig. 1) is activated by cyclin B (represented by Φ_0), forming a complex Cdc2-cyclin B (x). This complex activates its own activator Cdc25 (represented by the "+" loop), and also activates the Anaphase Promoting Complex (Y), which in turn promotes degradation of cyclin B

---

*Corresponding author: M. Chaves. The authors are with COMORE, INRIA, 2004 Route des Lucioles, BP 93, 06902 Sophia Antipolis, France. Emails: {indiaye,mchaves,gouze}@sophia.inria.fr.

(degradation of Φ_0, as well as inactivation of x back to form x_0). Some remarkable experiments on the Cdc2-cyclin B have been performed by two groups, Pomerening et al [6], and Sha et al [8], which show that the Cdc2-cyclin B system does exhibit bistability, that is two stable steady states exist for the same concentration of cyclin B. Further work by Pomerening et al [7] shows that the auto-activation positive feedback (denoted "+" in Fig. 1) is necessary for sustained oscillations to occur. The models proposed in [6, 7] have around 10 variables and about 30 parameters. They behave as "integrate-and-fire" or "relaxation" oscillators, using the conjunction of positive and negative feedback loops.

Here, we consider smaller 2,3-dimensional models, which are also of the type known as relaxation oscillators, because the periodic orbit essentially evolves along two different branches of the x-nullcline, with fast jumps between the two branches of the x-nullcline. In other words, along each branch of the nullcline, x is near quasi-steady state, and jumps rapidly between the two "steady states" In [7] the importance of the auto-activation positive feedback for generating oscillations was studied. In this paper, the focus is on the role of the negative feedback loop and on the analysis of the relative timescales of the various biological processes that are needed to generate a "relaxation" oscillator.

The negative feedback is formed by the system denoted y in Fig. 1, whose output $Y = h(y)$ (for some appropriate function of y) contributes to the degradation of Φ_0 and x. In general, y may be an n-dimensional vector, representing the components in a regulatory module, for instance proteins and messenger RNAs in a genetic regulatory network or another signalling pathway. In the example studied throughout the paper, we will consider y to be a scalar variable and the output to be $Y = y$. Theoretical conditions on the parameters are provided, that guarantee an oscillatory behaviour as observed in [7]. First, under constant regulation (fixed y, Y), our analysis provides conditions on the parameters for the existence of bistable behaviour. Then, adding slowly varying protein-protein activity, conditions are given that guarantee the existence of a periodic orbit. Finally, a set of parameters for the model is identified from data reported in [6, 7], and it satisfies all the "fast/slow" theoretical conditions. The model analysis also suggests further experiments to confirm or not, the hypothesis that the Cdc2-cyclin B oscillatory behaviour is generated by a mechanism combining a positive feedback with a slowly varying negative loop (as posed also in [7]).

Recent work [9] uses a similar "fast/slow" idea to study a system coupling an n-dimensional monotone system with a slow varying 1-dimensional system. Conditions are given for the existence of periodic orbits. An example of a MAPK cascade is given. However, no parameter estimation from the data is performed in [6, 7] or [9]. Our present study of a reduced 2-dimensional model has the advantage that each variable can be fitted to the corresponding steady state and time series data, the fast/slow hypotheses checked, and a maximum of information extracted using a minimum of mathematical machinery.

2   Coupling fast signalling and slow regulatory modules

Our goal is to study the role of slow processes (such as a genetic network) in the regulation of a faster process (such as a signal transduction network). For simplicity, we will consider one slow variable y (representing a regulatory genetic network or slowly evolving protein-protein interactions), and one fast varying variable x which represents a common signal transduction network, such as a MAPK cascade [4, 5] (see Fig. 1). Thus there are in fact two forms of a protein X, inactive (x_0) and active (x), but the their total concentration is constant: $x_0 + x = X_{tot}$. If x is below a certain threshold (θ_2), y is only weakly activated. but once x increases above that threshold, y becomes fully activated. The slow variable is characterized by an increasing sigmoidal activation function and a linear degradation rate: this is also the mathematical form typically used to describe a transcription/translation process [1]. Our analysis is thus applicable to systems coupling signal transduction and gene expression, or other genetic-like processes. The fast variable is negatively regulated by the slow variable (y promotes degradation of x), but there is also a positive auto-regulation term ($\Phi(x)$), that is x increases depending on the available quantity of inactive X ($x_0 = X_{tot} - x$):

$$
\begin{aligned}
\dot{x} &= \Phi(x)(X_{tot} - x) - \gamma_1 y x, \\
\dot{y} &= V_2 \frac{x^m}{x^m + \theta_2^m} - \gamma_2 y.
\end{aligned}
\tag{1}
$$

The function Φ should be an increasing function of x, and in the rest of the paper we will choose one general form (see Section 2.1). In particular, we wish to study conditions under which the slower dynamics can induce oscillations in the system. Suppose that, for some fixed y (for y in some interval I_y), the equation for x admits multiple steady states, representing different modes of operation of the signal transduction network. Suppose also that, for y outside this interval I_y, only a single steady state for x exists. Then, as the regulatory network y changes slowly to exit the multistability interval, the x module will respond by jumping from one steady state to another. The positive auto-regulation feedback loop is essential to generate two stable states for x. Then the negative feedback loop is necessary to induce x to change between its two (stable) states. Conditions are given to guarantee (or not) the existence of oscillations. Finally, the oscillatory dynamics is important: here, we wish to study the case where x spends most of the time near one of its stable modes, and then responds to a slowly evolving y by rapidly switching to its other state. This dynamics will follow from appropriate hypotheses on the timescales of the different biological processes. The theorem of Poincaré-Bendixson will be used to establish the existence of oscillations - this is a standard result for 2-dimensional systems (see, for instance, [10]; a recent example of its use for establishing conditions for oscillations in chemical reaction networks can be found in [11]).

This kind of oscillatory systems has been mathematically studied before [10], but never really applied to estimate parameters from biological experimental data to verify that the fast/slow conditions hold. Another new aspect analyzed in this paper is the use of the slow/fast framework to obtain analytical estimates for the period of the orbit in terms of the parameters of the system. Several predictions can then be made, for instance, which parameter most affects the period and the time spent in each "steady state" or mode of operation.

2.1   The model

To study the system (1) we will next introduce a general form for function Φ. This is motivated by a model of the cell cycle oscillator studied in [6, 7]. Equations (1) can be viewed as a reduced model of the cell cycle oscillator: the protein x represents Cdc2-Cyclin , and the slow variable y represents the Anaphase Promoting Complex (or APC). An inactive form of Cdc2-Cyclin B is also considered, which satisfies $x_0 = X_{tot} - x$. The transformation of protein x_0 to its active form x is mediated by another protein, w, for which we will add a simple equation with a constant synthesis rate (k_s). A basal level or external input may also be added (w_0), resulting in an activation term $\Phi_0 = k_1(w_0 + w)$, as shown in Fig. 1. The auto-activation feedback loop will be of the form $V_1 \frac{x^n}{x^n + \theta_1^n} x_0$. The protein x activates module y (represented by the term $V_2 \frac{x^m}{x^m + \theta_2^m}$), and a linear degradation rate is assumed for y ($\gamma_2 y$). In turn, the module y regulates degradation of both proteins x and w, by proteolysis of w (terms $-\gamma_1 yx$ and $-\gamma_s yw$). Taking the total concentration of Cdc2 to be constant, $x_0 + x = X_{tot}$, the equations are given by:

$$\dot{w} = k_s - \gamma_s yw \tag{2}$$

$$\dot{x} = \left(k_1(w_0 + w) + V_1 \frac{x^n}{\theta_1^n + x^n} \right)(X_{tot} - x) - \gamma_1 yx \tag{3}$$

$$\dot{y} = V_2 \frac{x^m}{x^m + \theta_2^m} - \gamma_2 y. \tag{4}$$

All parameters are positive, and it is easy to see that the nonnegative orthant ($[0, \infty[\times [0, \infty[\times [0, \infty[$) is invariant for the system. We will study this system using the idea that each of the three model's components has a specific response timeframe, and the three are clearly distinct. In other words, it will be assumed that three distinct timescales are present in the system: the activating stimulus (w) has the faster timescale, followed by the signalling protein x, with an intermediately fast or "normal" timescale, and the regulatory model has the slowest timescale (see Table 1).

The difference between signalling and transcription/translation times is well documented by now [1]. Regarding the activation by w, for this system, the mechanism for regulation and balancing of cyclin B is apparently not yet clear. It is well established that cyclin B is hardly present up to G2/M phase, where it rapidly accumulates to high concentration and activates Cdc2. At the end of mitosis, cyclin B is observed

to degrade rapidly, through proteolysis by APC. In our analysis we will assume that the time response of w is faster than that of x or y. We will treat this as an hypothesis, part of the model, to be confirmed or contradicted from the comparison of experimental data to the dynamical behaviour of the model arising from these hypotheses. In particular, it will be assumed from now on that w is at quasi-steady state, that is,

$$w = \frac{k_s}{\gamma_s}\frac{1}{y} = a_1\frac{1}{y}, \tag{5}$$

for $y > 0$ (it will be shown that y is strictly positive). Taking a new variable $x \rightsquigarrow x/X_{tot}$ and setting also $\theta_i \rightsquigarrow \theta_i/X_{tot}$ $(i = 1, 2)$, the system becomes:

$$
\begin{aligned}
\dot{x} &= \left(k_1(w_0 + \frac{a_1}{y}) + V_1\frac{x^n}{\theta_1^n + x^n}\right)(1 - x) - \gamma_1 yx \\
\dot{y} &= V_2\frac{x^m}{x^m + \theta_2^m} - \gamma_2 y.
\end{aligned}
\tag{6}
$$

A similar system was studied in [12] (with $a_1 = 0$), and it was shown that, for each fixed y, there are at most three and at least one steady states for x. It is not difficult to check that this is still true for the present x equation (see Fig. 2).

Although details are given for the cdc2-cyclin B system, model (2)-(4) can also be used to describe other biological systems. Consider, as another example, the NFκB-IκB network [3]. The transcription factor NFκB is present in the cytoplasm ($w =$NFκB$_{cyt}$) and in the nucleus ($x =$NFκB$_{nuc}$), where it activates transcription of the iκB gene ($y =$IκB mRNA). The protein IκB will bind NFκB, thus preventing its transcriptional activity ($\gamma_1 yx, \gamma_s yw$). Active and inactive forms of NFκB can be considered (x, x_0). Several other feedback loops exist (notably, through anti-apototic proteins such as IAP), which can be summarized by the positive auto-regulatory term $V_1\frac{x^n}{x^n+\theta_1^n}$. With these components, model (2)-(4) also describes oscillations in the NFκB-IκB network.

2.2 Different timescales

Following the biologically reasonable assumption that the dynamics of the signalling network is faster than the dynamics of the protein-protein regulatory module, we can rewrite the model under a standard slow/fast approach (under a fast time): $\dot{x} = f(x, y)$ and $\dot{y} = \gamma_2 g(x, y)$ with γ_2 small (see A1). Normalizing variable y to:

$$\widetilde{y} = \gamma_2\frac{y}{V_2},$$

system (6) can be rewritten as:

$$
\begin{aligned}
\frac{dx}{dt} &= \left(k_1(w_0 + \frac{\gamma_2}{V_2}\frac{a_1}{\widetilde{y}}) + V_1\frac{x^n}{x^n + \theta_1^n}\right)(1 - x) - \gamma_1\frac{V_2}{\gamma_2}\widetilde{y}x \\
\frac{d\widetilde{y}}{dt} &= \gamma_2\left(\frac{x^m}{x^m + \theta_2^m} - \widetilde{y}\right)
\end{aligned}
\tag{7}
$$

with the additional hypothesis that $\frac{\gamma_1}{\gamma_2}V_2 \gg \gamma_2$ (see Table 1).

The variable w can also be normalized with respect to some appropriate value, W_{tot}:

$$\widetilde{w} = \frac{w}{W_{tot}}, \quad \tilde{k}_s = \frac{k_s}{W_{tot}},$$

to obtain

$$\frac{d\widetilde{w}}{dt} = \tilde{k}_s\left(1 - \frac{\gamma_s}{\tilde{k}_s}\frac{V_2}{\gamma_2}\widetilde{y}\widetilde{w}\right).$$

The parameter $\tilde{k}_s$ should be large to justify the quasi-steady state assumption (5). Note that $a_1 = \frac{\tilde{k}_s}{\gamma_s}$. From the normalized equations, it follows that there will be three distinct timescales in system (2)-(4) if the parameters satisfy the constraints listed in Table 1.

4

Table 1: Timescales of the model's components.

Component	Timescale	Assumptions
Activation, w	fast	$\frac{k_s}{W_{tot}} \gg k_1 w_0 + V_1; \gamma_s \gg \gamma_1$
Signalling, x	normal	
Regulation, y	slow	$\gamma_2 \ll \min\{k_1 w_0 + V_1, V_2 \frac{\gamma_1}{\gamma_2}\}$

3 Stability analysis

The steady states of system (6) can be found by looking at the intersection between the nullclines $f(x, y) = 0$ and $g(x, y) = 0$. These can be solved with respect to y to obtain:

$$f_0(x) = \frac{1}{2\gamma_1} A(x) + \frac{1}{2\gamma_1} \sqrt{A(x)^2 + 4k_1 a_1 \gamma_1 \frac{1-x}{x}},$$

$$g_0(x) = \frac{V_2}{\gamma_2} \frac{x^m}{x^m + \theta_2^m},$$

where

$$A(x) = \left(k_1 w_0 + V_1 \frac{x^n}{\theta_1^n + x^n} \right) \frac{1-x}{x}.$$

The form of $f_0(x)$ depends on the values of the parameters. For instance, it can be strictly decreasing, or it can have an increasing region in between two decreasing regions (as depicted in Fig. 3). The y nullcline is always a strictly increasing function. If f_0 is strictly decreasing, it is not difficult to check that there is only one (stable) steady state. Here we will focus on the case of f_0 with three monotonic regions, as in Fig. 3. In addition, V_2, γ_2, and m will be assumed such that g_0 intersects f_0 only once. The stability of this unique steady state depends on which region g_0 and f_0 intersect (as shown below). Thus, the system will be studied under the following assumptions on the parameters:

A1. $\gamma_2 < \min\{\frac{1}{2}, \frac{3}{4} \frac{k_1(w_0 + a_1)}{\gamma_1 V_2}\}$ and $\gamma_2 \ll \frac{\gamma_1}{\gamma_2} V_2$;

A2. m is sufficiently large;

A3. there exist $0 < x_{\min} < x_{\max}$ with $df_0/dx(x_{\min}) = df_0/dx(x_{\max}) = 0$, $df_0/dx > 0$ for all $x \in]x_{\min}, x_{\max}[$, and $df_0/dx < 0$ for all $x \notin [x_{\min}, x_{\max}]$;

A4. $f_0(x_{\max}) < \max(g_0)$ (or $f_0(x_{\max}) < \frac{V_2}{\gamma_2}$, when m tends to infinity);

A5. $f_0(x_{\min}) > \min(g_0)$ (or $f_0(x_{\min}) > 0$, when m tends to infinity);

A6. $n \geq \frac{24}{V_1(1-\theta_1)} \left(2 \frac{a_1 \gamma_1}{w_0} \frac{\theta_1}{1-\theta_1} + k_1 w_0 + V_1 \right)$.

These assumptions guarantee that system (6) has the form necessary to exhibit oscillations. More precisely: A1 guarantees that the y equation is slow relative to the x equation (see Table 1); A2 guarantees that the activation of y by x is sufficiently steep to be fairly well approximated by a step-like function (this is used later in Section 5 to compute an analytical expression for the period of the orbit); A3 establishes the existence of a bistability region by saying that f_0 increases in $]x_{\min}, x_{\max}[$ and decreases in $[0, x_{\min}]$ and $[x_{\max}, 1]$ (see Figs. 2 and 3). If the function f_0 is strictly decreasing, then system (6) has only one stable steady state, and no oscillations are possible. If there is a region where f_0 is increasing then system (6) may have an unstable steady state and a periodic orbit, as will be shown (Fig. 3, middle). The values $x_{\min}$, $x_{\max}$ can in fact be viewed as an interval for the y activation threshold θ_2. Estimates for $x_{\min}$, $x_{\max}$ will be given in Lemma 3.4, with the help of assumption A6; A4 and A5, together with A2, guarantee that system (6) has

exactly one steady state, given by the intersection of the two nullclines f_0 and g_0. The "flat" parts of the y nullcline should not intersect the x nullcline (see Fig. 3):

$$x > \theta_2 : \quad g_0(x) \approx V_2/\gamma_2 > f_0(x_{\max})$$
$$x > \theta_2 : \quad g_0(x) \approx 0 < f_0(x_{\min}).$$

Finally, A6 says that n should be sufficiently large to generate a bistability region. It is used in Lemma 3.4 to find explicit conditions on the parameters to satisfy A3. But it is a conservative assumption: smaller n also satisfy the conditions.

First, we show that there are forward-invariant regions for both 3-dimensional and reduced systems. A set $\mathcal{D} \in \mathbb{R}^n$ is forward-invariant for a system $\dot{x} = f(x)$ if: for all $x_0 \in \mathcal{D}$, the solution $x(t)$ of the initial value problem $\dot{x} = f(x)$, $x(0) = x_0$ satisfies $x(t) \in \mathcal{D}$ for all $t \geq 0$.

Lemma 3.1 Assume A1 holds. Then the compact set

$$\mathcal{C} = \left[\frac{1}{2} \frac{k_s}{\gamma_1} \frac{\gamma_2}{V_2}, 4 \frac{k_s}{\gamma_1} \frac{\gamma_2}{V_2} \frac{\gamma_2^{2m} + \theta_2^m}{\gamma_2^{2m}} \right] \times \left[\gamma_2^2, 1 \right] \times \left[\frac{V_2}{2\gamma_2} \frac{\gamma_2^{2m}}{\gamma_2^{2m} + \theta_2^m}, \frac{V_2}{\gamma_2} \right]$$

is a forward-invariant set for system (2)-(4). Furthermore, the quasi-steady state approximation (5) is well defined in $\mathcal{C}$ and

$$\mathcal{D} = \left[\gamma_2^2, 1 \right] \times \left[\frac{V_2}{2\gamma_2} \frac{\gamma_2^{2m}}{\gamma_2^{2m} + \theta_2^m}, \frac{V_2}{\gamma_2} \right]$$

is a forward-invariant set for the reduced system (6).

Proof. To determine whether a given domain $\mathcal{D}$ is forward-invariant, we evaluate the vector field on the boundary of the domain. If the vector field points towards the interior of $\mathcal{D}$, then $\mathcal{D}$ is invariant. To check that $\mathcal{C}$ is a forward-invariant set for (2)-(4), it is clear that $\frac{dx}{dt} < 0$ whenever $x = 1$, and $\frac{dy}{dt} \leq 0$ whenever $y = \frac{V_2}{\gamma_2}$. It is also easy to check that $\frac{dw}{dt}(w_l, x, y) > 0$ whenever $w_l = \frac{1}{2} \frac{k_s}{\gamma_1} \frac{\gamma_2}{V_2}$ and $(w_l, x, y) \in \mathcal{C}$, or $\frac{dw}{dt}(w_r, x, y) < 0$ whenever $w_r = 4 \frac{k_s}{\gamma_1} \frac{\gamma_2}{V_2} \frac{\gamma_2^{2m} + \theta_2^m}{\gamma_2^{2m}}$ and $(w_r, x, y) \in \mathcal{C}$. For $y = y_l = \frac{V_2}{2\gamma_2} \frac{\gamma_2^{2m}}{\gamma_2^{2m} + \theta_2^m}$, using $x \geq \gamma_2^2$ it is clear that

$$\frac{dy}{dt}(w, x, y_l) > V_2 \frac{\gamma_2^{2m}}{\theta_2^m + \gamma_2^{2m}} - \gamma_2 \frac{V_2}{2\gamma_2} \frac{\gamma_2^{2m}}{\gamma_2^{2m} + \theta_2^m} > 0.$$

for all $(w, x, y_l) \in \mathcal{C}$. Finally, using assumption A1, one can choose γ_2 sufficiently small such that (setting $x_l = \gamma_2^2$, and using $y \leq V_2/\gamma_2$):

$$\frac{dx}{dt}(w, x_l, y) > \left(k_1 w_0 + V_1 \frac{\gamma_2^{2n}}{\theta_1^n + \gamma_2^{2n}} \right) (1 - \gamma_2^2) - \gamma_1 \frac{V_2}{\gamma_2} \gamma_2^2 > \frac{3}{4} k_1 w_0 - \gamma_1 V_2 \gamma_2 > 0$$

for all $(w, x_l, y) \in \mathcal{C}$, using $\gamma_2 > 0$ and $\gamma_2 < 1/2$ for the first inequality, and $\gamma_2 < \frac{3}{4} \frac{k_1(w_0 + a_1)}{\gamma_1 V_2}$ for the second inequality. Hence, the domain $\mathcal{C}$ is invariant.

To prove the second part of the Lemma, since y is strictly positive (and remains inside a strictly positive closed interval), the quasi-steady state approximation (5) is well defined in $\mathcal{C}$. Note that $\mathcal{D}$ is the projection of $\mathcal{C}$ on (x, y), and a similar proof shows that $\mathcal{D}$ is indeed invariant for system (6). ∎

The next result shows that system (6) has a unique equilibrium in $\mathcal{D}$, and analyses its stability.

Lemma 3.2 Assume A1-A5 hold. Then system (6) has a unique steady state, (x^*, y^*), and (a) if $\theta_2 \notin [x_{\min}, x_{\max}]$, then (x^*, y^*) is stable; (b) if $\theta_2 \in]x_{\min}, x_{\max}[$ then (x^*, y^*) is unstable.

6

Proof. Assumptions A2, A4 and A5 imply that f_0 and g_0 intersect at a single point (x^*, y^*) (as depicted in Fig. 3). To analyse stability of the steady state, consider the Jacobian. The following relations can be deduced from the nullclines'equations:

$$\frac{\partial f(x,y)}{\partial x} + \frac{\partial f(x,y)}{\partial y}s_1 = 0$$

$$\frac{\partial g(x,y)}{\partial x} + \frac{\partial g(x,y)}{\partial y}s_2 = 0, \tag{8}$$

where $s_1 = \frac{df_0}{dx}(x^*)$ and $s_2 = \frac{dg_0}{dx}(x^*)$ are the slopes of nullclines f_0 and g_0 computed at the steady state. Then the Jacobian is given by

$$J = \begin{bmatrix} \partial f/\partial x & \partial f/\partial y \\ \partial g/\partial x & \partial g/\partial y \end{bmatrix} = \begin{bmatrix} -s_1\partial f/\partial y & \partial f/\partial y \\ -s_2\partial g/\partial y & \partial g/\partial y \end{bmatrix}.$$

For a system of second order, it is well known that, if $\mathrm{tr}J < 0$ and $\det J > 0$ then the steady state is stable. In contrast, $\mathrm{tr}J > 0$ and $\det J > 0$ imply that the steady state is unstable. For both cases (a) and (b) it holds that $\det J > 0$. To see this, note that

$$\det J = (s_2 - s_1)\frac{\partial f}{\partial y}\frac{\partial g}{\partial y}$$

so $\det J > 0$ iff $s_2 > s_1$. This is always true for parameter sets satisfying A1-A5: for $\theta_2 \notin [x_{\min}, x_{\max}]$, it follows that $s_1 < 0 < s_2$; for $\theta_2 \in]x_{\min}, x_{\max}[$, with m large enough, it follows that $s_2 > s_1 > 0$. To check the sign of the trace of J, note that

$$\mathrm{tr}J = -s_1\frac{\partial f}{\partial y} + \frac{\partial g}{\partial y} = s_1\gamma_1 x^* - \gamma_2.$$

For case (a), $s_1 < 0$ so clearly $\mathrm{tr}J < 0$ and the steady state is stable. For case (b), $s_1 > 0$ but note that $x^* > x_{\min}$, where $x_{\min}$ is independent of γ_2 (since obtained from $df_0/dx = 0$). Thus, using assumption A1, one can choose γ_2 sufficently small such that $\gamma_2 < s_1\gamma_1 x_{\min} < s_1\gamma_1 x^*$. Thus, for case (b) the steady state is unstable. ∎

The dynamical behaviour of system (6) in case (b) can be further characterized (see also Fig. 5).

Lemma 3.3 Assume A1-A5 hold. If $\theta_2 \in]x_{\min}, x_{\max}[$, then system (6) admits a periodic orbit.

Proof. The existence of a periodic orbit follows immediately from the theorem of Poincaré-Bendixson [10] and the previous lemmas. The following two conditions are verified: (i) there exists a bounded, invariant region in the xy-plane ($\mathcal{D}$, Lemma 3.1); and (ii) this region contains a unique unstable steady state (Lemma 3.2). ∎

Finally, we will give sufficient conditions on the parameters for the system to verify assumption A3, and hence exhibit a periodic orbit. It is not easy to find explicit expressions for $x_{\min}$ and $x_{\max}$ in terms of the parameters of the system. To solve this problem, we will instead show that there exists $\Delta > 0$ such that the interval $I = [(1 - \Delta)\theta_1, \theta_1] \subset]x_{\min}, x_{\max}[$. In this case, a sufficient condition for existence of an unstable equilibrium point is $\theta_2 \in [(1 - \Delta)\theta_1, \theta_1]$.

Lemma 3.4 Let $\alpha = 1/2^{\frac{1}{n}} \in [\frac{1}{2}, 1]$ and suppose assumption A6 holds. Then $x_{\min} < \alpha\theta_1$ and $x_{\max} > \theta_1$.

Proof. To prove this, it is sufficient to verify that, for n large enough, the derivative of f_0 is positive for $x = \lambda\theta_1$ for any $\lambda \in [\alpha, 1]$, and becomes negative somewhere outside this interval. This follows from assumption A6 and the expression of the derivative of f_0:

$$\frac{df_0}{dx} = \frac{1}{2\gamma_1}\frac{dA}{dx} + \frac{1}{2\gamma_1}\frac{1}{c}\left(2A\frac{dA}{dx} - 4k_1a_1\gamma_1\frac{1}{x^2}\right),$$

where c denotes the expression: $\sqrt{A(x)^2 + 4k_1 a_1 \gamma_1 \frac{1-x}{x}}$. Note that $\frac{dA}{dx} < 0$ implies $\frac{df_0}{dx} < 0$ and that

$$\frac{dA}{dx} > 0 \text{ and } A\frac{dA}{dx} > 2k_1 a_1 \gamma_1 \frac{1}{x^2} \tag{9}$$

implies that $\frac{df_0}{dx} > 0$. For $x = \lambda\theta_1$ with $\lambda \leq 1$ obtain:

$$A(\lambda\theta_1) = \left(k_1 w_0 + V_1 \frac{\lambda^n}{\lambda^n + 1}\right)\frac{1 - \lambda\theta_1}{\lambda\theta_1}$$

$$\frac{dA}{dx}(\lambda\theta_1) = \frac{1}{\lambda^2\theta_1^2}\left(nV_1 \frac{\lambda^n}{(\lambda^n + 1)^2}(1 - \lambda\theta_1) - k_1 w_0 - V_1 \frac{\lambda^n}{\lambda^n + 1}\right).$$

Since $A(x)$ is positive for all x, to satisfy (9) it is sufficient that

$$n\lambda^n \geq 4\frac{2}{V_1(1 - \theta_1)}\left[2k_1 a_1 \gamma_1 \frac{\theta_1}{1 - \theta_1}\frac{1}{k_1 w_0} + k_1 w_0 + V_1\right]$$

$$\geq \frac{(\lambda^n + 1)^2}{V_1(1 - \lambda\theta_1)}\left[2k_1 a_1 \gamma_1 \frac{\lambda\theta_1}{1 - \lambda\theta_1}\frac{1}{k_1 w_0 + V_1\frac{\lambda^n}{\lambda^n + 1}} + k_1 w_0 + V_1 \frac{\lambda^n}{\lambda^n + 1}\right],$$

where we have used that fact that $1/2 \leq \lambda < 1$ and the following inequalities:

$$4 > (\lambda^n + 1)^2, \quad 1 > \frac{\lambda^n}{\lambda^n + 1} > 0, \quad \frac{\theta_1}{1 - \theta_1} > \frac{\lambda\theta_1}{1 - \lambda\theta_1}.$$

Now, by assumption $\lambda \geq \alpha = 1/2^{\frac{1}{n}}$, which leads to:

$$n\lambda^n \geq n\alpha^n = \frac{n}{2} \geq \frac{12}{V_1(1 - \theta_1)}\left[2k_1 a_1 \gamma_1 \frac{\theta_1}{1 - \theta_1}\frac{1}{k_1 w_0} + k_1 w_0 + V_1\right],$$

where assumption A6 was used in the last inequality. Therefore, under the assumptions, conditions (9) are indeed both satisfied. ∎

4 Parameter identification

To illustrate the theoretical results we will use systems (2)-(4) and (6) as a simple model for the mechanism of Cdc2 activation by cyclin B. This is is known to function as an autonomous oscillator [6] in the progression from G2 to M phases in the early embryonic cell cycle of *Xenopus* oocytes.

Two types of experiments were performed by Pomerening and co-authors. In the first set of experiments [6], a non-destructible form of cyclin B was used, which is not subject to APC-mediated degradation. Cyclin B was used as a constant input to the system: *Xenopus* egg extracts were treated with different concentrations of cyclin B and allowed to reach a steady state. Bistability and hysteresis were observed. In the second set of experiments [7], the importance of the positive feedback loop is explored (represented by the x auto-regulation in our models), and cyclin B is not externally controlled as before. Simultaneous measurements of cyclin B and Cdc2-cyclin B activity are available. We will next use two sets of experimental data to estimate parameters for model (6), and then check whether these are compatible with the timescales' assumptions.

4.1 Bistability

The experiments reported in [6] (see, in particular, Fig. 3(c) of this reference) can be interpreted as the response x to *constant inputs* w. The data consists of steady state values of x, for each constant w. In Fig. 4, the hysteresis curve for steady states of Cdc2-cyclin B as a function of the input u is reproduced as white squares and black stars. Since a non-destructible form of cyclin B was used, in our 3-dimensional model, the

w equation becomes redundant, and the system is modeled by (3) and (4), with constant $w \equiv u$. According to our analysis, if x is at steady state, then we expect y *to remain fixed at some (unknown) value* y_0.

Under these hypotheses, model (2)-(4) can be reduced to the x equation, with a new parameter $\gamma_0 = \gamma_1 y_0$, to be estimated:

$$\dot{x} = \Phi(x) - \gamma_0 x = \left(k_1(w_0 + u) + V_1 \frac{x^n}{x^n + \theta_1^n} \right)(1 - x) - \gamma_0 x \qquad (10)$$

The input term for x is of the form $\Phi_0 = k_1(w_0 + u)$, where $u = [\delta 65 - \text{cyclin B}]$ represents the concentration of the non-destructible cyclin B (known), w_0 represents a basal concentration of cyclin B (unknown parameter), and k_1 is the corresponding reaction rate.

A set of parameters that describe the biological system can be estimated by minimizing the difference between the data and the model's steady states. However, since the data consists of steady state measurements, it contains no information on the rapidity of convergence to steady state. That is, only the ratios V_1/k_1 and γ_0/k_1 can be obtained from the data. Observe also that, for large n, it is not possible to derive an explicit expression for the steady states of (10). Therefore, for the purposes of parameter estimation, we have chosen to approximate the sigmoidal expression $\frac{x^n}{x^n + \theta_1^n}$ by a ramp function (see also [12]). For simplicity, the exponent n will be fixed at $n = 4$. The estimation procedure is described in the Appendix, and further details given in the Supplementary material. As u varies from 0 to 40 nM, there should be only a "low" steady state; for u roughly in the interval 45 - 70 nM there should be both a "low" and a "high" steady state; finally, for u larger than 75nM there should be only a "high" steady state. For the existence of a bistability region, there are two possible cases for the "low" and a "high" stable steady states. The estimated parameters are given in Table 2.

Table 2: Estimated parameters. The errors indicated correspond to the diameter of a 95% confidence region for the bistability data, and 95% confidence intervals for the time series data.

Bistability Cdc2 activity data	
Parameter	Value
w_0	61.92 ± 1.74 nM
$\frac{V_1}{k_1}$	430.86 ± 4.09 nM
$\frac{\gamma_0}{k_1}$	843.42 ± 5.06 nM
θ_1	0.2752 ± 0.0012
n	4

Simultaneous Cdc2 activity, Cyclin B data	
Parameter	Value
w_0	19.78 ± 3.57 nM
a_1	1.504 ± 0.208 nM^2
k_1	$3.769 \times 10^{-4} \pm 3.92 \times 10^{-6}$ nM^{-1}min^{-1}
V_1	0.162 ± 0.0032 min^{-1}
V_2	0.251 ± 0.069 nM min^{-1}
γ_1	0.358 ± 0.09 nM^{-1}min^{-1}
γ_2	0.026 ± 0.0051 min^{-1}
θ_2	0.269 ± 0.045

4.2 Oscillations

One of the experiments reported in [7] (namely, Fig. 1V of this reference) shows the simultaneous evolution of both cyclin B (w) and Cdc2-cyclin B activity (x) (in a wild type case), but there are no APC measurements (y). Under the different timescales hypothesis, we consider that cyclin B responds much faster than Cdc2 to changes in APC, obtaining reduced system (6).

The parameters already obtained from the bistability data will now be used in the estimation of the remaining parameters, as follows:

- $\theta_2 \in [(1 - \Delta)\theta_1, \theta_1]$ (see Appendix);

- to simplify computational work, we choose and fix $m = 6$;

- γ_1 is newly estimated (since γ_0 is in fact $\gamma_1 y_0$, with unknown y_0);

- w_0 is newly estimated, since basal levels may depend on the experimental conditions;

- a_1, V_2, and γ_2 are newly estimated;

- k_1 is newly estimated; based on it the parameter V_1 can be computed.

The estimation procedure is a nonlinear least squares method, where the cost to be minimized is the difference between data points and model trajectories, both normalized to their maximal values (see Appendix). As before, this procedure was implemented in Matlab 7.3, using the function `lsqnonlin`. The parameters obtained are shown in Table 2, and the final fit may be seen in Fig. 4.

4.3 Validation of different timescales hypotheses

Estimates have now been obtained for all parameters of (2-dim) system (6). To check whether the assumptions on the timescales are verified recall that (Table 1):

$$\gamma_2 \ll \min\{k_1 w_0 + V_1, \frac{\gamma_1}{\gamma_2}V_2\}: \quad 0.026 \pm 0.0051 \ll \min\{0.17, 1.54\}.$$

Assumption A1 further requires:

$$\gamma_2 < \frac{3}{4}\frac{k_1(w_0 + a_1)}{\gamma_1 V_2}: \quad 0.026 \pm 0.0051 < 0.034.$$

We have considered the error bars for each parameter to find the minimum values of $k_1 w_0 + V_1$, $\frac{\gamma_1}{\gamma_2}V_2$, and $\frac{k_1(w_0+a_1)}{\gamma_1 V_2}$. Since we have no way to access γ_s or k_s/W_{tot}, it cannot be checked whether the quasi-steady state assumption on w is justified. However, looking at the data in Fig. 4, we observe that cyclin B ($= w$) has a fairly constant value during the sharp increase in Cdc2-cyclin B ($= x$) (the symbols 'o' in the time interval [75,85] minutes). According to the model, y remains pratically constant during the sharp x rise (see also Fig. 5). This argues in favor of the approximation $w \approx a_1/y$.

The estimated parameters satisfy all inequalities. These results indicate that system (2), together with the hypotheses of substantially different timescales is a reasonable model of the Cdc2-cyclin B oscillator. This 2-dimensional model may have the disavantage of being too schematic and not containing enough detail, but many advantages are also gained: it is suitable for parameter estimation from the available measurements, avoiding many problems related to underdetermined systems; and it still provides a faithful and useful phenomenological description of the biological system.

5 Period, sensitivity analysis and more experiments

Assume now that conditions A1-A6 are satisfied, and system (6) has a periodic orbit. To obtain some knowledge on the period of the orbit, as well as its dependence on the various parameters, we will again use the "fast/slow" variables assumptions. The partial state y (regulation variable) represents a variable whose evolution is slow relative to x (signalling variable). As an example, consider the parameters obtained for the cdc2-cyclin B system and the corresponding trajectories (Fig. 5 (a),(b)). It can be observed that x switches rapidly between two ("steady") states or two distinct modes of operation of x: x remains for some time (roughly around 50s) on a low concentration state (x_B), before rapidly jumping to a high concentration state (x_A). The time spent in the high state is much shorter (roughly around 7s), and then x quickly falls back to x_B. In contrast, the variable y responds slowly to changing x concentration. (y evolves according to decreasing or increasing negative exponentials). In the phase space (Fig. 5 (a)), this fast/slow dynamics is seen by the fact that the periodic orbit moves practically along the $y = f_0(x)$ nullcline as y decreases from its maximal to minimal value: along this nullcline, $\dot{x} = 0$, so x remains practically constant in this part of the cycle (at x_A). This type of dynamics is more clearly illustrated in Fig. 5 (c),(d) (where two parameters are slightly changed from those in Table 2). Here, it is clear that the "slow" part of the system corresponds to changes in y with an almost constant x, as trajectories move along the x-nullcline ($y = f_0(x)$). The fast part of the system corresponds to rapid changes in x, as it jumps from one state to another in response to y.

5.1 Period of the orbit

Using the above arguments, the time spent by the system in each of the operation modes can be analytically estimated. Let:

$$T_1 = \text{ time spent in mode } x_B,$$
$$T_2 = \text{ time spent in mode } x_A.$$

During T_1, we assume that the trajectory evolves along the nullcline $y = f_0(x)$, with $x = x_B$. Moreover, the dynamics of y can be simplified: for large Hill coefficient m (assumption A2), the expression $V_2 x^m / (x^m + \theta_2^m)$ can be approximated by a step function with $s(x) = 0$ if $x < \theta_2$ and $s(x) = V_2$ if $x > \theta_2$. Then the y equation becomes

$$\frac{dy}{dt} \approx f_0'(x)\frac{dx}{dt} = \gamma_2 \left(\frac{V_2}{\gamma_2}\frac{x^m}{x^m + \theta_2^m} - f_0(x) \right) \approx -\gamma_2 f_0(x)$$

As x increases from x_B to x_A, integration gives:

$$T_1 = \frac{\ln f_0(x_A) - \ln f_0(x_B)}{\gamma_2}.$$

During T_2, we assume once more that the trajectories are close to the $y = f_0(x)$ nullcline, and let $G(x) = \frac{V_2}{\gamma_2} - f_0(x)$ to obtain:

$$f_0'(x)\frac{dx}{dt} = \gamma_2 G(x) \Rightarrow \int_{x_B}^{x_A} \frac{f_0'(x)}{G(x)} dx = \int_0^{T_2} \gamma_2 dt$$

and integration gives:

$$T_2 = \frac{\ln G(x_B) - \ln G(x_A)}{\gamma_2}.$$

Following Lemma 3.4, we approximate $x_B \approx (1 - \Delta)\theta_1$ and $x_A \approx \theta_1$ to obtain:

$$T_1 \approx \frac{1}{\gamma_2} \ln \frac{f_0(\theta_1)}{f_0((1 - \Delta)\theta_1)} \approx 29.2,$$

$$T_2 \approx \frac{1}{\gamma_2} \ln \frac{\frac{V_2}{\gamma_2} - f_0((1 - \Delta)\theta_1)}{\frac{V_2}{\gamma_2} - f_0(\theta_1)} \approx 3.0.$$

These analytical formulas are interesting for several reasons:

- the ratio between T_1 and T_2 gives an idea of the fraction of time spent by the system on each of its stable operation modes (x_A or x_B). In the example, $T_1/(T_1 + T_2) \approx 0.94$ meaning that the oscillator remains 94% of its cycle with relatively low concentrations of active Cdc2-cyclin B;

- it is often difficult to obtain analytical estimates for the period of a periodic orbit, but these formulas give an indication (see Fig. 6): using the different timescales hypotheses, the system could be simplified enough to write down an approximate analytical expression. However, if the hypotheses are not strongly satisfied, there can be a large difference between the analytical estimates and the real perid. For the parameters in Table 2, we have $(T_1 + T_2)$/Period=$\approx 27.55/79.76 = 0.34$, an error of 66%. As the difference between timescales becomes more marked, the sum $T_1 + T_2$ will provide better estimates, and their sum gives a reasonable estimate of the full cycle period (with errors as low as 7%, as seen in Fig. 2 in the Supplementary material). The quality of the $T_1 + T_2$ estimate depends on how well the values $f_0(x_B) = f_0((1 - \Delta)\theta_1)$ and $f_0(x_A) = f_0(\theta_1)$ approximate the actual value of y as x jumps between low and high levels;

- these formulas show how each parameter will influence the value of T_1, T_2 and hence the period of the orbits (Fig. 6).

A sensitivity analysis of the time duration $T_1 + T_2$, and the total period of the orbit is shown in Fig. 6. Only one parameter was varied at a time, with all others fixed at their estimated values shown in Table 2. Each parameter p was varied in an interval: $[0.85p, 1.15p]$ (i.e., between a 15% decrease and increase to its original value). The total period was computed by simulating the system with the new set of parameters, while $T_1 + T_2$ was directly computed from the (approximated) analytical formulas. Note that $T_1 + T_2$ is indeed a good predictor of the changes in the period in response to changes in each parameter: a variation in the period is always captured by a similar variation in $T_1 + T_2$. For a 15% perturbation in each parameter a periodic orbit still exists, except in the case of θ_2. Indeed, for small values of θ_2, there is no periodic orbit, and the system converges to a steady state (not shown). This is in agreement with Lemma 3.3 which provides an interval for θ_2 which guarantees existence of oscillations, and Lemma 3.2 which says that, outside that interval, there exists a stable fixed point.

5.2 Model predictions and experiments

The positive auto-regulation is a very important component of the model, since this is the component responsible for the existence of two stable steady states (for fixed y), and hence two distinct stable modes of operation for system (6) (Section 2.1). Recall that this positive feedback is represented by the term $V_1 x^n / (x^n + \theta_1^n)$, so that V_1 is the strength of the auto-regulation effect.

Interestingly, analysis of the expression $T_1 + T_2$ shows that it is inversely proportional to all parameters, except V_1 (Fig. 6). For instance, for the Cdc2-cyclin B oscillator (fixing all parameters as in Table 2), the model predicts a 10% increase in $T_1 + T_2$ in response to a 15% increase in V_1.

In [7], the effect of the positive regulation was studied experimentally, by attempting to "break" the loop. This was achieved by adding a non-phosphorylatable form of Cdc2, thus decreasing the strength of the positive regulation. The average period observed for the wild type Cdc2-cyclin B oscillator was around 80 mins., while the modified system had a shorter period, around 55 mins. (Fig. 2 in [7], and Table 3 below). This, indeed, agrees with the model's predictions for a 40% reduction in the strength of the auto-regulatory loop.

Table 3: Influence of the positive feedback on the period.

System	Experiment [7]	Model	Parameters
Wild type Cdc2	80 mins	79.76 mins	as in Table 2
Non-phosphorylated Cdc2 (weaker positive feedback)	55 mins	55.6 mins	$\tilde{V}_1 = 0.57 V_1$

Another prediction of the model is that V_2 influences only T_2, the time spent in x_A (the high concentration state). Thus is it possible to obtain a modified dynamics, for instance by forcing the periodic orbit to spend the same amount of time in each operation mode, simply by decreasing V_2. This is illustrated in Fig. 5 (c) and (d), with $\tilde{V}_2 = 0.15 V_2$. This suggests a new experiment to check whether the oscillatory mechanism of Cdc2-cyclin B is generated by a model of the type (6). By increasing the rate of synthesis of y, does the firing-peak duration increase, that is can one observe similar orders of magnitude for the durations T_1 and T_2? This would correspond to a situation where the cyclin B-Cdc2 oscillator spends similar amounts of time in each of its two modes, x_A and x_B (respectively, at high and low concentrations of Cdc2-cyclin B complex). If all other parameters are unchanged, this will also increase the period of oscillations.

6 Conclusions

It is well known that different biological processes may have very distinct timescales (for instance, transcription or translation are typically slower than signalling events). Here we have studied a possible dynamical outcome induced by the interconnection between biological modules whose response times are substantially

different. We proposed and analysed a mechanism through which slowly varying regulation patterns (such as genetic-like) can induce rapid changes in the mode of operation of signal transduction networks, and thus lead to sustained oscillations (a system of the class usually refered to as "relaxation oscillators"). Under appropriate assumptions on the timescales (there are "fast", "normal", and "slow" variables), explicit sufficient conditions on the parameters are provided, for the existence of a periodic orbit. This mechanism is illustrated by an application to the Cdc2-cyclin B oscillator. Using experimental data reported in [6, 7] a set parameters was identified, which satisfies all the different timescales hypotheses.

These results suggest the following interpretation of the dynamics of cyclin B in the Cdc2-cyclin B oscillator. From the biological point of view, it is well established that cyclin B is hardly present up to G2/M phase, where it rapidly accumulates to high concentration and activates Cdc2. At the end of mitosis, cyclin B is observed to degrade rapidly, through proteolysis by APC, However, there appear to be many uncertainties still on the process of cyclin B synthesis and balancing. Our study suggests that cyclin B follows very rapidly the dynamics of APC (or group of proteins related to this phase). Since this regulation module has a slower timescale, cyclin B would appear to also evolve slowly, until a sufficient concentration of APC is available to degrade it. Thus, cyclin B is possibly regulated by protein products from the APC phase. Our results also suggest possible candidates (for components y), based on its activation threshold: $\theta_2 \in [(1 - \Delta), 1]\theta_1$.

A further experiment suggested by our analysis is to increase the rate of synthesis of products y. The prediction is that the high concentration peak in active Cdc2-cyclin B complex will broaden, so the system will spend more time in its high Cdc2-cyclin B concentration state. The system would then switch rapidly between its two modes of operation (while spending similar lengths of time in each of these).

Finally, we would like to emphasise that this study presents a simple, very schematic model, which has the advantages of being intuitive and amenable to analytical theoretical analysis. In this way, we were able to generate conditions on the parameters that guarantee a desired dynamical behaviour. Furthermore, since available data consists essentially of the measurements of two variables, a 2-dimensional model is also more suitable for parameter estimation, in the sense that each of the model's variables can be compared to data, and the most information extracted using a minimum of mathematical machinery. The model has the advantage of providing a faithful phenomenological description and thus suggest possible experiments to further understand the dynamical mechanisms of the biological oscillator.

7 Acknowledgements

References

[1] U. Alon. *An introduction to systems biology*. Chapman & Hall/CRC, Boca Raton, 2007.

[2] G. Lahav, N. Rosenfeld, A. Sigal, N. Geva-Zatorsky, A.J. Levine, M. Elowitz, and U. Alon. Dynamics of the p53-Mdm2 feedback loop in individual cells. *Nat. Genetics*, 36:147–150, 2004.

[3] A. Hoffmann, A. Levchenko, M.L. Scott, and D. Baltimore. The IkB-NFkB signaling module: temporal control and selective gene activation. *Science*, 298:1241–1245, 2002.

[4] B. N. Kholodenko. Negative feedback and ultrasensitivity can bring about oscillations in the mitogen-activated protein kinase cascades. *Eur. J. Biochem.*, 267:1583–1588, 2000.

[5] J.E. Ferrell and W. Xiong. Bistability in cell signalling: how to make continuous processes discontinuous, and reversible processes irreversible. *Chaos*, 11:227–238, 2001.

[6] J.R. Pomerening, E.D. Sontag, and J.E. Ferrell. Building a cell cycle oscillator: hysteresis and bistability in the activation of Cdc2. *Nat. Cell Biol.*, 5:346–351, 2003.

[7] J.R. Pomerening, S.Y. Kim, and J.E. Ferrell. Systems-level dissection of the cell-cycle oscillator: bypassing positive feedback produces damped oscillations. *Cell*, 122:565–578, 2005.

[8] W. Sha, J. Moore, K. Chen, A.D. Lassaletta, C.-S. Yi, J.J. Tyson, and J.C. Sible. Hysteresis drives cell-cycle transitions in *Xenopus laevis* egg extracts. *Proc. Natl. Acad. Sci USA*, 100:975–980, 2003.

[9] T. Gedeon and E.D. Sontag. Oscillations in multi-stable monotone systems with slowly varying feedback. *J. Differential Equations*, 239:273–295, 2009.

[10] L. Perko. *Differential equations and dynamical systems*. Springer, Berlin, 2001.

[11] J. Coatleven and C. Altafini. A kinetic mechanism inducing oscillations in simple chemical reactions networks. In *Proc. 47th IEEE Conf. Decision and Control*, Cancun, Mexico, 2008.

[12] I. Ndiaye, M. Chaves, and J.-L. Gouzé. Study and parameter identification of a model coupling cell signaling and gene expression. In *Proc. 16th Mediterranean Conf. Control and Automation (MED'08)*, Ajaccio, France, 2008.

A Parameter estimation details

A.1 Bistability

To obtain analytic explicit expressions for the "high" and "low" steady states the function Φ in (10) is approximated as follows:

$$\Phi(x) \approx \begin{cases} \Phi_l(x) = \Phi_0(1-x), & x < (1-\Delta)\theta_1 \\ \Phi_m(x) = \left(\Phi_0 + \frac{V_1}{2\Delta\theta_1}(x - (1-\Delta)\theta_1)\right)(1-x), & (1-\Delta)\theta_1 \leq x \leq (1+\Delta)\theta_1 \\ \Phi_r(x) = (\Phi_0 + V_1)(1-x), & x > (1+\Delta)\theta_1, \end{cases} \quad (11)$$

where $\Delta = 2/n$ and $\Phi_0 = k_1(w_0 + u)$. Using this approximation, the steady states of (10) as functions of the input u can be obtained by finding the solutions to:

$$\Phi_l(x) = \gamma_0 x, \quad \Phi_m(x) = \gamma_0 x, \quad \text{or} \quad \Phi_r(x) = \gamma_0 x.$$

The "low" steady state is always given by the intersection of the line $\gamma_0 x$ with the left branch $\Phi_l(x)$:

$$\bar{x}_{\text{low}}(u) = \frac{w_0 + u}{w_0 + u + \frac{\gamma_0}{k_1}} \quad \in [0, (1-\Delta)\theta_1) \quad (12)$$

Then the line $\gamma_0 x$ intersects the middle branch $\Phi_m(x)$ at least once, giving rise to an unstable steady state. (See Fig. 1 in the Supplementary material.) The "high" steady state $\bar{x}_{\text{high}}(u)$ can be given by a second intersection of $\gamma_0 x$ with $\Phi_m(x)$:

$$\bar{x}_{\text{high}}^m(u) = \max\left\{\frac{-c_1 \pm \sqrt{c_1^2 - 4c_0 c_2}}{2c_2}\right\} \quad \in [1-\Delta, 1+\Delta]\theta_1, \quad (13)$$

where $\Delta = 2/n$ and

$$c_0 = w_0 + u - \frac{1}{2\Delta\theta_1}\frac{V_1}{k_1}(1-\Delta)\theta_1,$$

$$c_1 = \frac{1}{2\Delta\theta_1}\frac{V_1}{k_1}(1 + (1-\Delta)\theta_1) - \left(w_0 + u + \frac{\gamma_0}{k_1}\right),$$

$$c_2 = -\frac{1}{2\Delta\theta_1}\frac{V_1}{k_1}.$$

Or it can be given by the intersection of $\gamma_0 x$ with the right branch $\Phi_r(x)$:

$$\bar{x}^r_{\text{high}}(u) = \frac{w_0 + u + \frac{V_1}{k_1}}{w_0 + u + \frac{V_1}{k_1} + \frac{\gamma_0}{k_1}} \in ((1+\Delta)\theta_1, 1],$$

To compare these expressions to the data there is another problem: recall that the variable x is normalized to is maximal value, X_{tot}, so any steady state satisfies $0 \leq \bar{x} \leq 1$. The data is given in terms of phosphorimager units, and there is no way to estimate X_{tot}. To avoid this problem, we have considered the data relative to the steady state at $u = 100$nM, and also normalized the model's steady. Since the data around $u = 100$nM seems messy (and after some preliminary numerical tests), we used the lowest possible value allowed by the error bar (white squares): $w^*_{100} = 220 - 60 = 160$. Thus the expressions to fit to the data are in fact:

$$\frac{\bar{x}_{\text{low}}(u)}{\bar{x}_{\text{high}}(100)}, \quad \frac{\bar{x}^m_{\text{high}}(u)}{\bar{x}_{\text{high}}(100)}, \quad \frac{\bar{x}^r_{\text{high}}(u)}{\bar{x}_{\text{high}}(100)}.$$

In addition, we can also estimate the bistability region $[u_{\min}, u_{\max}]$ from the data:

$$u = u_{\max} \;\Rightarrow\; \bar{x}_{\text{low}}(u_{\max}) = (1 - \Delta)\theta_1$$
$$u = u_{\min} \;\Rightarrow\; \bar{x}_{\text{high}}(u_{\min}) = \beta$$

where $\beta = (1 + \Delta)\theta_1$ or such that the two roots of the quadratic are equal, $\beta = \frac{-c_1}{2c_2}$. (See Fig. 1 in the Supplementary material.) Under these conditions the following parameters can be identified:

$$p(1) = \frac{V_1}{k_1}, \; p(2) = \theta_1, \; p(3) = \Delta, \; p(4) = \frac{\gamma_0}{k_1}, \; p(5) = w_0.$$

These parameters where estimated using the function `lsqnonlin` in Matlab (version 7.3) to minimize:

$$J(p) = 10 \sum_{i=\min,\max} \left| \frac{u_i - u_{obs,i}}{u_{obs,i}} \right|^2 + \sum_{u \in U} \left| \frac{\frac{\bar{x}(u)}{\bar{x}_{\text{high}}(100)} - \frac{w_u}{w^*_{100}}}{\frac{w_u}{w^*_{100}}} \right|^2$$

where $U = [0, 25, 40, 45, 50, 60, 75]$, w_u, $u_{obs,\min} = 42.5$, $u_{obs,\max} = 72.5$ denote the data points, $w^*_{100} = 160$ (see note above), and $\bar{x}(u)$ denotes the corresponding "low" or "high" steady state expression. The factor 10 multiplying the first sum aims to increase the weight of the error related to the bistability region, since this was a very important part of the modelling. The computation of the cost $J(p)$ includes an algorithm to verify which of the forms of $\bar{x}_{\text{high}}(u)$ is the correct one. More details, including sensitivity analysis for the optimized parameter set and a confidence region, can be found in the Supplementary material.

A.2 Oscillations

There were seven parameters to estimate from the data on cyclin B ($1/y$) and the cdc2-cyclin B (x) activity. The cost function to be minimized was

$$J_o(p(1), \ldots, p(7)) = J_o(\gamma_1, a_1, \theta_2, \frac{V_2}{\gamma_2}, \gamma_2, k_1, w_0) = 5J_x + J_y,$$

where a larger weight was assigned to J_x because preliminary experiments showed that typically $J_x < J_y$.

$$J_x(p) = \sum_{t \in T} \left| \frac{x(t)}{\max_{t \in T} x(t)} - \frac{W^c(t)}{\max_{t \in T} W^c(t)} \right|^2 \Big/ \left| \frac{W^c(t)}{\max_{t \in T} W^c(t)} \right|^2$$

$$J_y(p) = \sum_{t \in T} \left| \frac{1/y(t)}{\max_{t \in T} 1/y(t)} - \frac{W^B(t)}{\max_{t \in T} W^B(t)} \right|^2 \Big/ \left| \frac{W^B(t)}{\max_{t \in T} W^B(t)} \right|^2$$
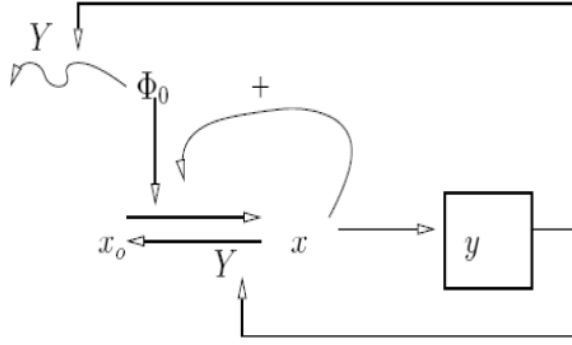
Figure 1: Simplified scheme of the mechanism of regulation.
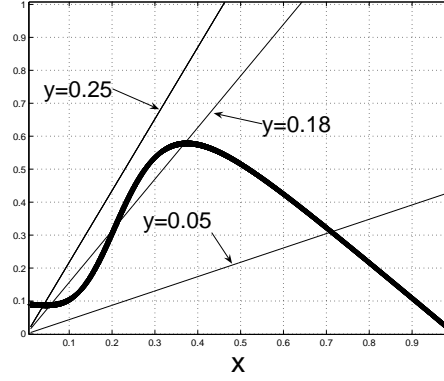

Figure 2: The bold curve represents $\Phi(x) = (\Phi_0 + V_1 \frac{x^n}{x^n + \theta_1^n})(1-x)$ and the other curves represent $\psi = \gamma_1 y x$ for three values of y, as indicated. Values of parameters: $\Phi_0 = 0.09$, $V_1 = 1$, $V_2 = 1.275 \times 10^{-2}$, $\gamma_1 = 8.7$, $\gamma_2 = 3.75 \times 10^{-2}$, $\theta_1 = 0.25$, $\theta_2 = 0.2$, $n = 4$, $m = 50$.

where $t \in \{22, 24, \ldots, 94\}$ (the data points used here start at $t = 22$, and are spaced 2mins apart), $W^c(t)$ denotes the concentration of cdc2-cyclin B, and $W^B(t)$ that of cyclin B. At each step of the optimization procedure, equations (6) were solved (using the current parameter set), and a "candidate" periodic orbit was detected. One period of this candidate orbit was then normalized to maximal values (both x and y), and the cost J_o was calculated. More details, including the covariance matrix and confidence intervals for the optimized parameter set, can be found in the Supplementary material.
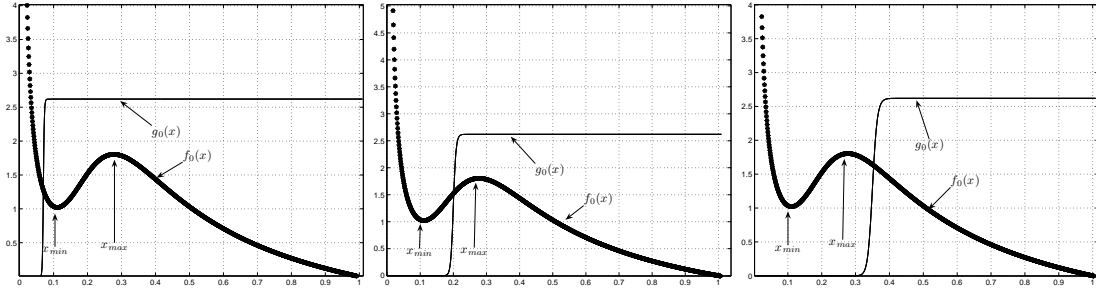
Figure 3: Representation of nullclines. By varying θ_2, one of two cases is obtained: either θ_2 belongs to the interval $]x_{\min}, x_{\max}[$ (middle); or θ_2 is outside the interval $[x_{\min}, x_{\max}]$, either below $x_{\min}$ (left), or above $x_{\max}$ (right). Parameters are as in Fig. 2 and (left to right) a) $\theta_2 = 0.07$, b) $\theta_2 = 0.2$, and c) $\theta_2 = 0.35$.
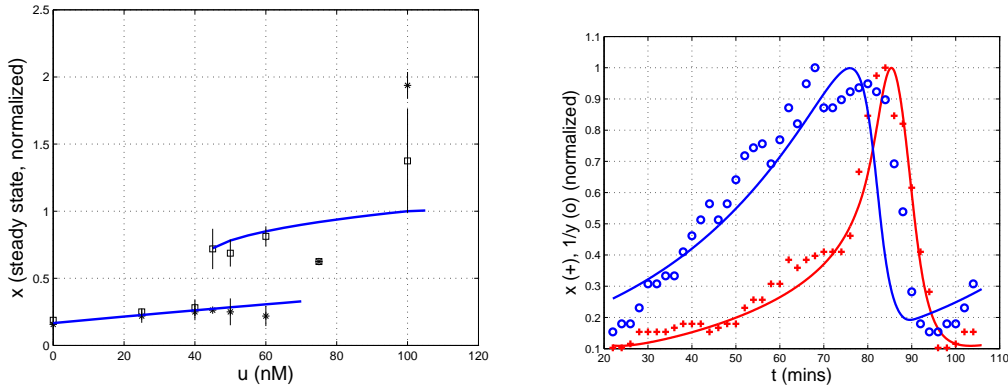

Figure 4: Data fitting. Left: steady state response of Cdc2-cyclin B activity. Solid lines represent expressions (12), (13) with parameters as in Table 2. The stars and squares represent the hysteresis data from Fig. 3(c) of [6]. Right: dynamical evolution of Cdc2-cyclin B activity ('+') and cyclin B ('o'). The symbols represent data from Fig. 1V of [7]. Solid curves represent the model variables, normalized to their maximal value. Variable x fits to '+' and $1/y$ fits to 'o'.
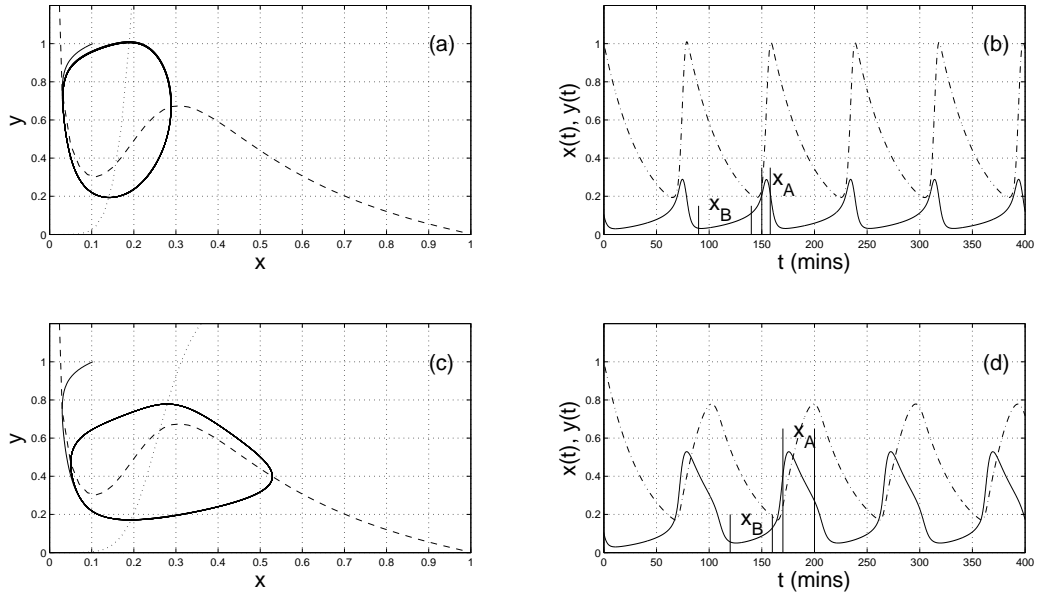
Figure 5: Periodic orbit and trajectories for system (6), with parameters as in Table 2 (a),(b), or with new $\tilde{V}_2 = 0.2V_2$ for (c),(d). In (a) and (c) the nullclines f_0 (dashed line) and g_0 (dotted line) are shown, together with one trajectory (solid line) in the phase plane. In (b) and (d) the same trajectory is shown as a function of time ($x(t)$ and $y(t)$ are represented, respectively, by the solid and dash-dotted lines).
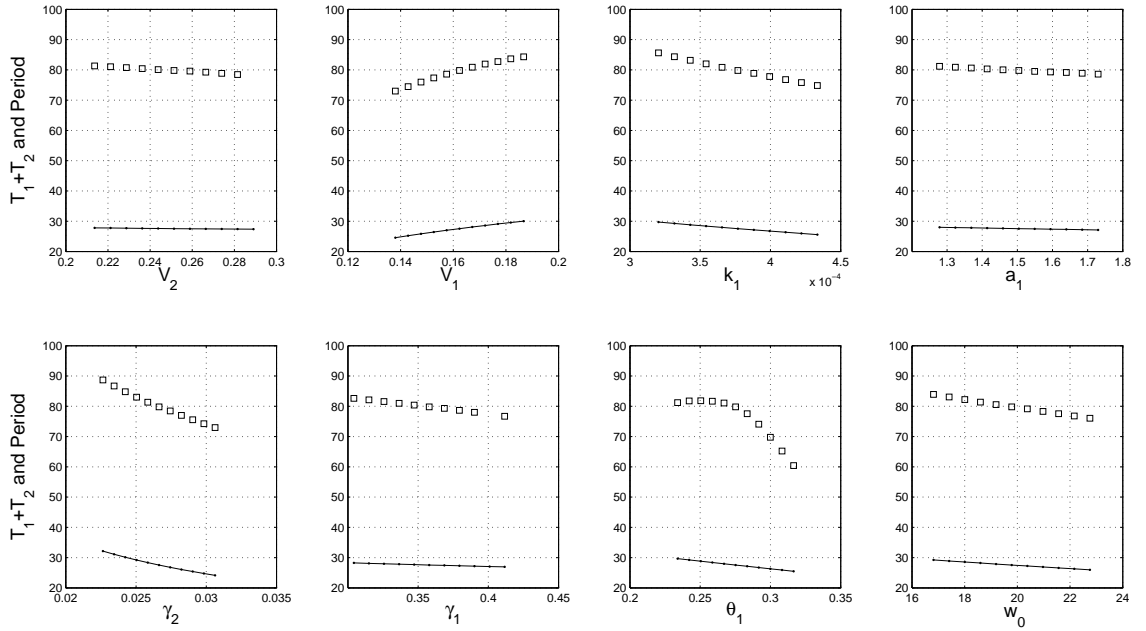

Figure 6: Sensitivity with respect to each parameter, for the period and the time intervals T_1, T_2. Each parameter was varied between 80% and 120% of its original value (only one parameter is varied at a time). The period (open squares) was numerically calculated from a simulation of the system. The values of T_1 and T_2 (solid lines with dots) where calculated directly from their formulas.

18